Available online at www.sciencedirect.com
ScienceDirect
Journal of Sound and Vibration 301 (2007) 391–399
JOURNAL OF SOUND AND VIBRATION
www.elsevier.com/locate/jsvi

Short Communication

Receiving radius determination in ray-tracing sound prediction of rectangular enclosure

Zhongjin Jiang[a,*], Xiaojun Qiu[b]

[a]State Key Laboratory of Millimeter Waves, Southeast University, Nanjing, 210096, China
[b]Institute of Acoustics, Nanjing University, Nanjing, 210093, PR China

Received 23 September 2005; received in revised form 8 May 2006; accepted 29 May 2006
Available online 28 December 2006

Abstract

In this paper, the ray-tracing sound prediction for the rectangular enclosure is researched, and a new method is proposed to determine the receiving radius by sound ray density. The sound ray density can be calculated based on the initial sound ray number, volume and shape of the enclosure, and the boundary absorption coefficient. In an established enclosure, the sound ray density can be regarded to be evenly distributed statistically, so the receiving radius should be constant and have no relation to the position in the enclosure. The sound ray density is variable for different sound spaces, so the receiving radius should also be variable for different enclosures. The higher is the sound ray density, the shorter the receiving radius is, and the lower is the sound ray density, the longer the receiving radius is. A formula of calculating the receiving radius in rectangular enclosure has been deduced in this paper. The results of the experiments and predictions show that the new reception model can predict the sound pressure level (SPL) and the reverberation time T_{30} accurately.

1. Introduction

The sound field prediction methods based on the geometric acoustics include ray-tracing method [1,2], image source method [3,4] and the combined ray-tracing and image source method [5]. The last one also has conical beam method [6] and triangular beam method [7]. The ray-tracing method is commonly used for its high accuracy in prediction and high efficiency in computation.

The receiving sphere is indispensable in the ray-tracing method, while how to determine its radius is still a problem needed to be researched. There are three kinds of reception model. In the first kind of model, the receiving radius is constant for different positions in an established sound space, and is also constant for different sound spaces. A widely applied example is the normal model [8–10], which has been used, in some commercial software, and the radius is usually 0.5 or 1.0 m [8,11]. In this model the relation among the receiving radius, sound space volume and initial sound ray number can be given as

$$r = \left(\frac{15V}{2\pi N}\right)^{1/3}. \tag{1}$$

*Corresponding author.

0022-460X/$ - see front matter © 2006 Elsevier Ltd. All rights reserved.
doi:10.1016/j.jsv.2006.06.047

Here r is the receiving radius, N the number of total initial sound rays, and V the volume of the space. This kind of radius cannot be fit for the sound spaces of arbitrary size, and Hilmar has discussed its systematic error [12,13].

In the second kind of model, the receiving radius is constant for different positions in an established sound space, but is variable for different sound spaces. A reception model of this kind is proposed in this paper and is applied in the sound prediction of rectangular enclosures.

In the third kind of model, the receiving radius is variable not only for different sound spaces, but also for different positions in an established sound space. A reception model of this kind was put forward by Hilmar [12], which gave the radius formula as following:

$$r = d\sqrt{\frac{2\pi}{N}} = ct\sqrt{\frac{2\pi}{N}}. \tag{2}$$

Here, d is the propagating distance of the sound ray, c the sound velocity and t the propagating time of the sound ray. The computation time of this method was considerably long because the receiving radius will be updated continuously as the sound rays propagate forward.

Another reception model of the third kind was proposed by Zeng [14], called Zeng's model here, and the formula of the receiving radius is given as following:

$$r = d_{\mathrm{SR}}\sqrt{\frac{4}{N}}\log_{10} V. \tag{3}$$

Here, d_{SR} means the distance from the sound source to the receiving point (source–receiver distance). The receiving radius of this model is proportional to the source–receiver distance, so the radius will be very large when the receiving sphere is far from the sound source, and the spatial resolution of prediction in the far field will be decreased.

In this paper, a new reception model of the second kind is proposed for sound prediction of the rectangular enclosure, and a formula is deduced to calculate the receiving radius in accordance with the sound ray density. In the ray-tracing prediction in this paper, the initial sound rays are uniformly emitted from the omni-directional source with prefixed elevation angle and azimuth angle, and the propagation of the sound rays includes specular reflection and diffuse reflection as in the Lambert diffusion model [15,16]. The ray trace is terminated according to the energy discontinuity percentage (EDP) but not the reflection number. The sound rays are detected by the receiving sphere to obtain the impulse response, from which the needed acoustical indexes can be calculated. While only the sound ray reception is discussed in detail in this paper.

2. Research of the new reception model

2.1. Relation between the sound ray density and the receiving radius

The sound field in an enclosure can be regarded to be reverberating when the enclosure shape is not apparently long or oblate, and the sound ray density is evenly distributed statistically. Though the density cannot be completely even for different positions, the density fluctuation is little and can be neglected. So in an established enclosure, the receiving radius is constant for different positions. While the sound ray density will be variable for different sound fields, so the receiving radius will also be variable for different enclosures.

In the new reception model in this paper, the receiving radius will be longer when the sound ray density is lower, otherwise no enough rays can be received and the statistical effect cannot be achieved. Meanwhile the radius will be shorter when the sound ray density is higher, otherwise the computational time will be very long and the spatial resolution of sound prediction will be decreased meaninglessly.

There are some factors, which have relation to the sound ray density as well as the receiving radius. The first one is of course the number of the initial sound rays. The second is the volume of the enclosure because larger volume can lead to smaller sound ray density. The shape, also the side ratio, of the enclosure is also an important factor because oblate enclosure can attenuate the sound field quickly. Finally, the absorption coefficient of the enclosure boundary should also be taken into consideration, because the sound will be

attenuated more quickly when the boundary absorption coefficient is greater. So the receiving radius should be calculated with these factors.

The influence of the absorption coefficient on the sound ray density depends on how to terminate the trace of a ray. In some ray-tracing models, the trace is terminated according to the reflection number, in which the sound ray density will not be influenced by the absorption coefficient. In other models, the trace is terminated according to the EDP, namely the threshold of the sound ray energy, in which the sound ray density will be influenced by the absorption coefficient. In this paper, the trace is terminated according to the EDP, which is more widely applied in ray-tracing prediction, so the absorption coefficient is used to calculate the sound ray density.

While the diffused coefficient and scattered coefficient need not be considered, because they have relation to the propagating path of the sound rays, while in an enclosed space, the sound ray density will still be statistically even and will not be changed.

2.2. Determination of the receiving radius in rectangular enclosure

A formula of the receiving radius can be deduced here based on the sound ray density. In an established rectangular space whose length, width and height are l, w and h, respectively, as shown in Fig. 1(a), the sound

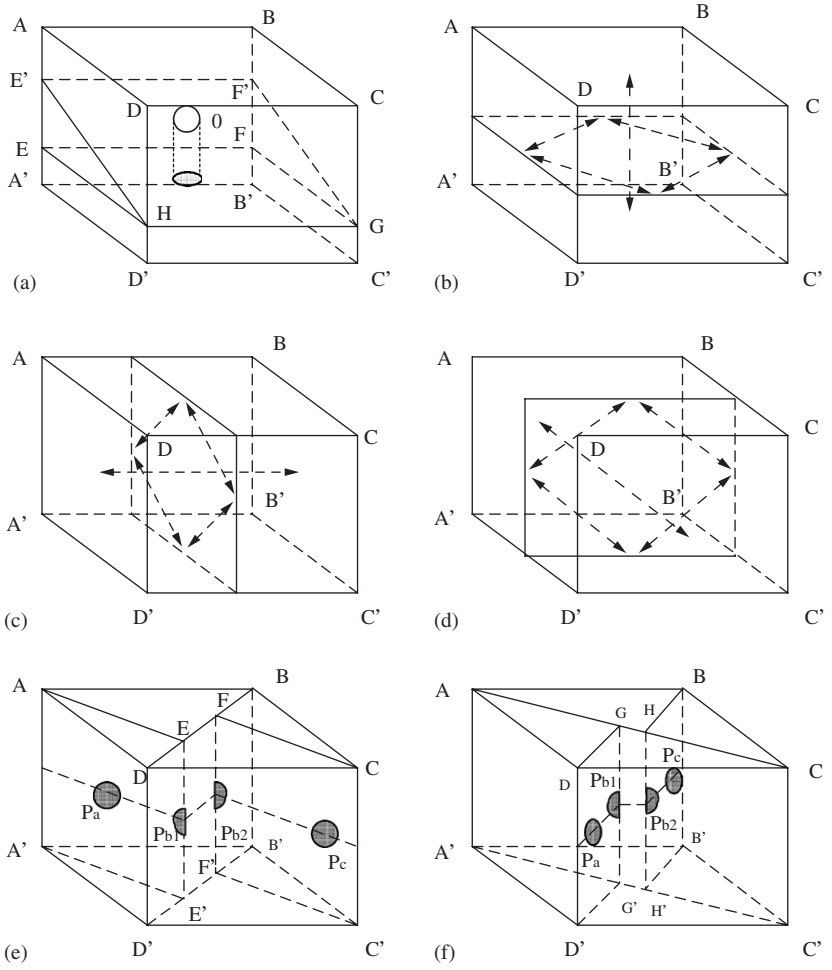

Fig. 1. Cross area and receiving area in a rectangular space: (a) cross area and receiving area between ABCD and A′B′C′D′; (b) the first team; (c) the second team; (d) the third team; (e), (f) cross area and receiving area between two adjacent planes.

rays are reflected in any direction disorderly and distributed evenly statistically. While it is sure that each ray will start from one plane and end at another plane, and there are many sound rays between every two planes. Because a rectangular space has six planes, there are totally 15 groups of sound ray, and each group starts and ends between certain two planes.

As shown in Fig. 1(a), the sound ray group between ABCD and A′B′C′D′ will pass through planes such as EFGH and E′F′GH, while the area of EFGH is the minimum one because it is vertical to AA′. Here, the area of EFGH is defined as the cross area of this sound ray group, called $S_{\text{P-EFGH}}$ here. The sphere O is the receiving sphere, and the gray district is its projection on EFGH. The area of the gray district is defined as the receiving area of this sound ray group, called $S_{\text{R-EFGH}}$ here. This is because the received round rays in this group will all pass through a circle in the receiving sphere whose area is the same as the $S_{\text{R-EFGH}}$. If the total sound ray number in this group is $N_{\text{P-EFGH}}$, and the received sound ray number in this group is $N_{\text{R-EFGH}}$, the sound ray density in this group can be defined as following:

$$\rho_{\text{EFGH}} = \frac{N_{\text{P-EFGH}}}{S_{\text{P-EFGH}}} = \frac{N_{\text{R-EFGH}}}{S_{\text{R-EFGH}}}. \tag{4}$$

Sound ray density means the number of sound rays passing through every unit cross area.

These 15 sound ray groups can be divided into three teams, and each team consists of five groups. The first team is demonstrated in Fig. 1(b) in which every bidirectional arrow represents a group, and this team consists of the group between ABCD and A′B′C′D′, between AA′B′B and BB′C′C, between BB′C′C and CC′D′D, between CC′D′D and DD′A′A, between DD′A′A and AA′B′B. In like manner, the second team and the third team are demonstrated in Fig. 1(c) and (d), respectively.

In the first team, for the sound ray group between ABCD and A′B′C′D′ (see Fig. 1(a)), the cross area $S_{\text{P-EFGH}}$ is wl. If the receiving radius is r, the receiving area $S_{\text{R-EFGH}}$ is πr^2.

When calculating the cross area between DD′A′A and AA′B′B in the first team (see Fig. 1(e)), AA′E′E is vertical to DD′B′B, so it is the cross area. In like manner, CC′F′F is the cross area between BB′C′C and CC′D′D. Their area can be calculated as following:

$$S_{\text{P-AA'E'E}} = S_{\text{P-CC'F'F}} = h\frac{wl}{\sqrt{w^2+l^2}}. \tag{5}$$

When calculating the receiving area between DD′A′A and AA′B′B altogether with the receiving area between BB′C′C and CC′D′D, the projection of the receiving sphere will move on AA′E′E and CC′F′F with the moving of the receiving sphere. The projection may be entirely on AA′E′E such as the gray district P_a, and also may be entirely on CC′F′F such as the gray district P_c. It is still possible that one part of the projection is on AA′E′E and the other part is on CC′F′F such as P_{b1} and P_{b2}. Therefore, it can be deduced that

$$S_{\text{R-AA'E'E}} + S_{\text{R-CC'F'F}} = \pi r^2. \tag{6}$$

In like manner, in the first team, the cross area between AA′B′B and BB′C′C is $S_{\text{P-BB}''_{\text{HH}}}$ (see Fig. 1(f)), and the cross area between CC′D′D and DD′A′A is $S_{\text{P-DD'G'G}}$, and they are both the same as $S_{\text{P-AA'E'E}}$. On the other hand, the receiving area between AA′B′B and BB′C′C is $S_{\text{R-BB'H'H}}$, the receiving area between CC′D′D and DD′A′A is $S_{\text{R-DD'G'G}}$, and the sum of $S_{\text{R-BB'H'H}}$ and $S_{\text{R-DD'G'G}}$ is still πr^2.

So far, the total cross area and the total receiving area in the first team can be calculated as

$$\begin{aligned} S_{\text{P-team1}} &= wl + 4\frac{wlh}{\sqrt{w^2+l^2}}, \\ S_{\text{R-team1}} &= 3\pi r^2. \end{aligned} \tag{7}$$

In like manner, the total cross area and the total receiving area in the second team can be calculated as

$$\begin{aligned} S_{\text{P-team2}} &= wh + 4\frac{wlh}{\sqrt{w^2+h^2}}, \\ S_{\text{R-team2}} &= 3\pi r^2. \end{aligned} \tag{8}$$

The total cross area and the total receiving area in the third team can be calculated as

$$S_{\text{P-team3}} = lh + 4\frac{wlh}{\sqrt{l^2+h^2}},$$
$$S_{\text{R-team3}} = 3\pi r^2. \tag{9}$$

The total cross area and the total receiving area in the space can be calculated as following:

$$S_p = wl + wh + lh + \frac{4wlh}{\sqrt{w^2+l^2}} + \frac{4wlh}{\sqrt{w^2+h^2}} + \frac{4wlh}{\sqrt{l^2+h^2}},$$
$$S_R = 9\pi r^2. \tag{10}$$

Because the sound rays distribute evenly in the rectangular space, the sound ray density in every group is regarded to be the same to each other. Therefore, if the total number of the sound rays in the space is N_p and the total number of received sound rays is N_R, the sound ray density in the space can be calculated as

$$\rho = \frac{N_{p-1}}{S_{p-1}} = \frac{N_{p-2}}{S_{p-2}} = \cdots = \frac{N_{p-15}}{S_{p-15}} = \frac{N_{p-1}+N_{p-2}+\cdots+N_{p-15}}{S_{p-1}+S_{p-2}+\cdots+S_{p-15}} = \frac{N_p}{S_p} = \frac{N_R}{S_R}. \tag{11}$$

Here, N_{p-i} and S_{p-i} mean the sound ray number and cross area, respectively, in the ith group.

In ray-tracing method, the reflection order M_{ref} can be calculated as following:

$$(1-a)^{M_{\text{ref}}} = C_{\text{th}},$$
$$M_{\text{ref}} = \log_{1-a} C_{\text{th}}. \tag{12}$$

Here C_{th} is the tracing threshold, and α is the space boundary absorption coefficient. The total number of the sound rays N_p is the product of M_{ref} and the initial sound ray number N

$$N_p = NM_{\text{ref}} = N\log_{1-a} C_{\text{th}}. \tag{13}$$

The sound ray density can be calculated as

$$\rho = \frac{N\log_{1-a} C_{\text{th}}}{wl + wh + lh + \frac{4wlh}{\sqrt{w^2+l^2}} + \frac{4wlh}{\sqrt{w^2+h^2}} + \frac{4wlh}{\sqrt{l^2+h^2}}} = \frac{N_{\text{R}}}{9\pi r^2}. \tag{14}$$

The receiving radius can be calculated based on above formula

$$r = \sqrt{\frac{N_{\text{R}}\left(wl + wh + lh + \frac{4wlh}{\sqrt{w^2+l^2}} + \frac{4wlh}{\sqrt{w^2+h^2}} + \frac{4wlh}{\sqrt{l^2+h^2}}\right)}{9\pi N\log_{1-a} C_{\text{th}}}}$$
$$= \sqrt{\frac{N_{\text{R}}\left(\frac{S}{2} + 4V\left(\frac{1}{\sqrt{w^2+l^2}} + \frac{1}{\sqrt{w^2+h^2}} + \frac{1}{\sqrt{l^2+h^2}}\right)\right)}{9\pi N\log_{1-a} C_{\text{th}}}}. \tag{15}$$

In above formula, S means the surface area of the rectangular enclosure and is related to the enclosure shape. V is the volume of the rectangular enclosure. So the receiving radius has relation to the number of the initial sound rays, the volume and shape of the enclosure, and the absorption coefficient of the boundaries.

2.3. Calculation of the sound pressure level

In the ray-tracing prediction, all the sound rays arriving at the receiving sphere can be detected, and their sound intensity and arriving time can be worked out. The sound intensity of the ith sound ray I_i can be

calculated as following [8,14]:

$$I_i = \frac{W_i d_{ri}}{V_r}. \tag{16}$$

Here, W_i is the power of the ray when it arrives the sphere, d_{ri} the distance of the sound ray passing through the receiving sphere, and V_r the volume of the receiving sphere. The sound intensity of different sound rays can be sequenced according to their arriving time so to obtain the impulse response $I(t)$.

The SPL can be calculated from the impulse response as [14]

$$\mathrm{SPL} = 10\log_{10}\left(\frac{p_e^2}{4\times 10^{-10}}\right) = 10\log_{10}\left(\frac{\rho_0 c_0 \int_0^\infty I(t)\,\mathrm{d}t}{4\times 10^{-10}}\right). \tag{17}$$

The propagating medium in this paper is air, and the $\rho_0 c_0$ can be taken to be $400\,\mathrm{kg\,m^{-2}\,s^{-1}}$, so the SPL can be calculated as

$$\mathrm{SPL} = 120 + 10\log_{10}\left(\int_0^\infty I(t)\,\mathrm{d}t\right). \tag{18}$$

This algorithm has been widely applied in different reception models.

3. Experiment results

The performance of the normal model, Zeng's model and the new reception model proposed in this paper, called Jiang's model here, are compared with each other. The SPL and reverberation time T_{30} in two rectangular enclosures are measured and predicted with the above three reception models. One enclosure is the reverberation chamber of the Institute of Acoustics Nanjing University, and the other enclosure is a common rectangular room. The rectangular room has more complicated structure because it has two windows and an ordinary wooden door on the wall. The purpose of choosing this room is to test the application of the new reception model in a common room.

The width, length and height of the reverberation chamber are 5.91, 7.34 and 5.27 m, respectively, and the width, length and height of the rectangular room are 4.52, 5.43 and 3.41 m, respectively. The volume and shape of the two enclosures are both different from each other. The boundary absorption coefficients of the two enclosures are given in Table 1, for the octave bands from 125 to 4000 Hz. The reverberation chamber has smooth concrete walls, while the rectangular room has lime-coated walls so with greater absorption coefficient. For each enclosure there were totally 9 test points, and their coordinates and source–receiver distances are given in Table 2, altogether with the coordinate of the sound source.

In the measurement the used apparatus was B&K Pulse-3560D system, which can generate and receive signals. The sound source was a directional loudspeaker and the wideband noise of 0–5 KHz was used as the test signal.

In the prediction the number of the initial sound rays N was 25,000. The tracing threshold C_{th} and the received sound ray number N_R were set to be 0.001 and 1500, respectively. The tracing threshold should be less than 0.01 [11], or the prediction accuracy will not be satisfactory. N_R 500, 1000, 1500, 2000, 2500 were all tested in simulation to compare the prediction accuracy, and 1500 was the most proper one. Too small N_R cannot meet the need of statistical computation, while too large N_R will result in a too big receiving sphere and decrease the spatial resolution of the sound prediction.

Table 1
Boundary absorption coefficients of the two enclosures

Reverberation chamber						
Frequency (Hz)	125	250	500	1000	2000	4000
a	0.012	0.015	0.017	0.020	0.025	0.035
Rectangular room						
Frequency (Hz)	125	250	500	1000	2000	4000
a	0.025	0.030	0.035	0.040	0.050	0.070

Table 2
Coordinate of the sound source and the test points (d_{SR} means the source–receiver distance)

	Source	Points								
		1	2	3	4	5	6	7	8	9
Reverberation chamber										
X (m)	0.6	1.5	3.0	1.0	4.5	3.0	4.5	1.6	4.5	3.0
Y (m)	0.8	1.8	1.8	3.6	1.8	3.6	3.6	5.6	5.4	5.9
Z (m)	0.5	2.0	1.0	1.5	2.0	3.5	1.6	3.8	1.0	4.7
d_{SR} (m)	0.0	2.01	2.65	3.00	4.30	4.75	4.93	5.91	6.05	7.03
Rectangular room										
X (m)	0.6	1.5	2.0	2.5	2.5	3.0	3.5	3.5	4.0	4.0
Y (m)	0.8	2.0	2.0	3.0	2.0	3.0	4.0	4.0	5.0	5.0
Z (m)	0.5	1.0	2.0	1.0	3.0	2.0	1.0	3.0	2.0	3.0
d_{SR} (m)	0.0	1.58	2.38	2.95	3.36	3.58	4.35	4.99	5.61	5.95

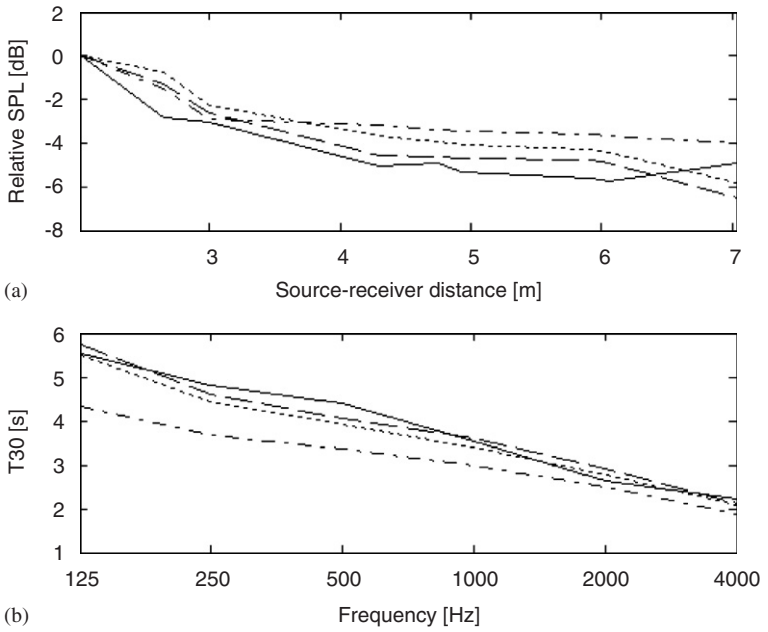

Fig. 2. Measured and predicted results in the reverberation chamber. (——, the measured result; – – – –, the predicted result of the Jiang's model; . . . . ., the predicted result of the Zeng's model; – – – –, the predicted result of the normal model): (a) measured and predicted relative SPL; (b) measured and predicted T_{30}.

The measured and predicted relative SPL in the reverberation chamber are given in Fig. 2(a). At each test point, the relative SPL of 500 and 1000 Hz are measured and predicted to get the average value. From the figure, the SPL decreases with the source–receiver distance. This is mainly because the direct sound is radiate in the space, so the SPL further from the sound source is inevitably lower even in a reverberation chamber. When comparing the three predicted results, the result of the Jiang's model is most close to the measured result, and the result of the Zeng's model is better than that of the normal model. The prediction error of the normal model, the Zeng's model and the Jiang's model are 1.2957, 1.1157 and 0.7418 dB, respectively.

The measured and predicted T_{30} in the reverberation chamber are compared with each other in Fig. 2(b). The prediction and measurement were performed at the 9 test points for the octave bands from 125 to 4000 Hz. At every frequency, the T_{30} given in the figure is the average T_{30} of the 9 test points. From the figure it can be seen that the Jiang's model can present better performance than the other tow models. The prediction

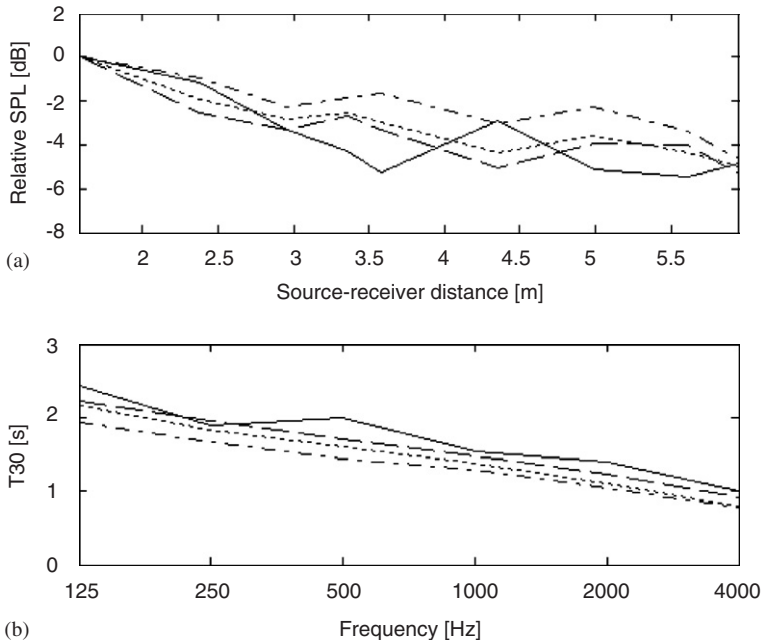

Fig. 3. Measured and predicted results in the rectangular room (——, the measured result; – – – –, the predicted result of the Jiang's model; . . . ., the predicted result of the Zeng's model; – – – –, the predicted result of the normal model): (a) measured and predicted relative SPL; (b) measured and predicted T_{30}.

error of the Normal model, the Zeng's model and the Jiang's model are 0.7293, 0.2239 and 0.1991 s, respectively.

The measured and predicted relative SPL in the rectangular room are given in Fig. 3(a). As talked above, the SPL at each test point is the average SPL of 500 and 1000 Hz. The Zeng's model can present a lightly better performance than the Jiang's model, and these two models are both better than the normal model. The prediction error of the normal model, the Zeng's model and the Jiang's model are 1.3868, 1.0625 and 1.1370 dB, respectively. When compared with Fig. 2(a), there is obvious fluctuation in the relative SPL along the source–receiver distance because the rectangular room has a more complicated space structure.

The measured and predicted T_{30} in the rectangular room are given in Fig. 3(b). The T_{30} at each frequency is the average T_{30} of the 9 test points. The Jiang's model can predict the reverberation time more accurately than the other two models, and the Zeng's model is better than the Normal model. The prediction error of the Normal model, the Zeng's model and the Jiang's model are 0.3577, 0.2384 and 0.1428 s, respectively. When comparing Fig. 2(b) and Fig. 3(b), T_{30} in the rectangular room is obviously less than that in the reverberation chamber; this is because the rectangular room has greater boundary absorption coefficient and smaller volume than the reverberation chamber.

4. Conclusions

For an established enclosure, the receiving radius should be constant for different positions, because the sound ray density can be taken to be evenly distributed statistically. While the radius should be variable for different enclosures because the sound ray density is variable for different sound fields. In the new reception model the radius is determined by the number of the initial sound rays, the volume and shape of the enclosure, and the boundary absorption coefficient. According to the experiment and simulation results for different rectangular enclosures, this new model can predict SPL and T_{30} accurately.

The new reception model is established theoretically based on optimal rectangular enclosure, in which the sound field is reverberating. While according to the experiment results in the rectangular room, it can also be applied to sound prediction for common rooms. The new reception model is useful for complicated enclosures

like an auditorium if the enclosure meets two conditions. First, the complicated enclosure should be approximately square, so its length, width and height can be estimated. Secondly the sound field in it should be reverberating and the sound energy should be evenly distributed.

Acknowledgments

The work is supported by Jiangsu Postdoctoral Scientific Research Supporting Plan, China Postdoctoral Science Foundation (2004036414) and Project 10304008 supported by NSFC and SRF for ROCS, SEM and SRFDP.

References

[1] A. Krokstad, S. Strom, S. Sorsdal, Calculating the acoustical room response by the use of a ray tracing technique, *Journal of Sound and Vibration* 8 (1968) 118–125.
[2] A. Kulowski, Algorithmic representation of the ray-tracing technique, *Applied Acoustics* 18 (1985) 449–469.
[3] R. Heinz, Binaural room simulation based on an image source model with addition of statistical method to include the diffuse sound scattering of walls and to predict the reverberation tail, *Applied Acoustics* 38 (1993) 145–159.
[4] H. Lee, B.H. Lee, An efficient algorithm for the image model technique, *Applied Acoustics* 24 (1988) 87–115.
[5] I.A. Drumm, Y.W. Lam, The adaptive beam-tracing algorithm, *Journal of the Acoustics Society of America* 107 (2000) 1405–1412.
[6] M. Vorlander, Simulation of the transient and the steady-state sound propagation in rooms using new combined ray-tracing/image source algorithm, *Journal of the Acoustics Society of America* 81 (1989) 172–176.
[7] T. Lewers, A combined beam tracing and radiant exchange computer model of room acoustics, *Applied Acoustics* 38 (1993) 161–178.
[8] L.N. Yang, B.M. Shield, Development of a ray tracing computer model for the prediction of the sound field in long enclosure, *Journal of Sound and Vibration* 229 (2000) 133–146.
[9] S.M. Dance, B.M. Shield, The effect on prediction accuracy reducing the number of rays in a ray-tracing model, *Inter-Noise* 94 (3) (1994) 2127–2130.
[10] A.M. Ondet, J.L. Barbry, Modeling of sound propagation in fitted workshops using ray tracing, *Journal of the Acoustics Society of America* 85 (1989) 787–796.
[11] L.N. Yang, B.M. Shield, The prediction of speech intelligibility in underground stations of rectangular cross section, *Journal of the Acoustics Society of America* 109 (2001) 266–273.
[12] H. Lehnert, Systematic errors of the ray trace algorithm, *Applied Acoustics* 38 (1993) 207–221.
[13] H. Lehnert, J. Blauert, Principles of binaural room simulation, *Applied Acoustics* 38 (1992) 259–291.
[14] X.Y. Zeng, K.A. Chen, J.C. Sun, On the accuracy of the ray-tracing algorithms based on various sound receiver models, *Applied Acoustics* 64 (2003) 433–441.
[15] B. Dalenback, Room acoustics prediction based on a unified treatment of diffuse and specular reflection, *Journal of the Acoustics Society of America* 100 (1996) 899–909.
[16] X.Y. Zeng, K.A. Chen, J.C. Sun, Development of a hybrid computer model for simulating the virtual sound field in enclosure, *Applied Acoustics* 63 (2002) 481–491.